Plasma afterglow circulation apparatus for decontamination of spacecraft equipment

Meike Müller, Tetsuji Shimizu, Sylvia Binder, Petra Rettberg, Julia L. Zimmermann, Gregor E. Morfill, and Hubertus Thomas

Citation: AIP Advances **8**, 105013 (2018); doi: 10.1063/1.5040303
View online: https://doi.org/10.1063/1.5040303
View Table of Contents: http://aip.scitation.org/toc/adv/8/10
Published by the American Institute of Physics

Plasma afterglow circulation apparatus for decontamination of spacecraft equipment

Meike Müller,[1,a] Tetsuji Shimizu,[2] Sylvia Binder,[3] Petra Rettberg,[4] Julia L. Zimmermann,[3] Gregor E. Morfill,[3] and Hubertus Thomas[1]
[1]*Deutsches Zentrum für Luft- und Raumfahrt e.V., Institut für Materialphysik im Weltraum, Arbeitsgruppe Komplexe Plasmen, Münchener Str., 82234 Weßling, Germany*
[2]*Electronics and Photonics Research Institute, National Institute of Advanced Industrial Science and Technology, Umezono 1-1-1, Tsukuba 305-8568, Japan*
[3]*terraplasma GmbH, Lichtenbergstraße, 85748 Garching bei München, Germany*
[4]*Deutsches Zentrum für Luft- und Raumfahrt e.V., Institut für Luft- und Raumfahrtmedizin, Linder Höhe, 51147 Köln, Germany*

(Received 16 May 2018; accepted 2 October 2018; published online 10 October 2018)

A newly developed apparatus using cold atmospheric plasma (CAP) is presented, providing a useful alternative decontamination method for spacecraft equipment. The designed setup uses the plasma afterglow generated by a surface micro-discharge (SMD) technology and works with a circulating gas flow of ambient air at room temperature. Additionally, the apparatus allows the control of gas flow, plasma power and humidity, and offers O_3 monitoring and a variable treatment volume. Within this study we examined the apparatus' performance by evaluation of the inactivation efficacy of bacterial endospores *Bacillus atrophaeus* in different treatment volumes of 0.54 l, 1.8 l and 2.6 l. The experiments with *Bacillus atrophaeus* showed at least a 4.4 log reduction after the treatment times of 10, 20 and 30 min in the respective treatment chambers with a volume of 0.54 l, 1.8 l and 2.6 l. These results demonstrate that high sporicidal effects can be achieved with the newly developed apparatus, and that longer treatment times are needed for larger treatment volumes due to different filling rates of reactive components in different treatment volumes. Conclusively, these investigations illustrate the scalability of the designed apparatus up to 2.6 l for the afterglow treatment of samples with flat surfaces. The composition of the plasma afterglow was analysed by Fourier Transformation Infrared (FTIR) and UV absorption spectroscopy. The spectroscopic analyses identify O_3, N_2O, and HNO_3 as predominant products of the CAP apparatus. https://doi.org/10.1063/1.5040303

I. INTRODUCTION

In space research the exploration of the outer space and the search for extra-terrestrial life are of great interest. In order to protect the explored extra-terrestrial bodies from terrestrial organisms and to prevent backward contamination in the case of earth return missions,[1–3] the Committee on Space Research (COSPAR) created planetary protection policies. COSPAR provides an international standard for spacefaring nations and defined five categories of missions to avoid harmful contamination in space exploration.[1] Previous publications demonstrated that a microbial diversity inhabit spacecraft assembly clean rooms despite their extreme environment.[4,5] In particular, spore forming bacteria like *Bacillus* species can outlast nutrient poor conditions, and germinate when favourable conditions are restored. Some of these species were observed in spacecraft associated environments[3,4] and could become a potential risk for planetary protection.[6–9] This robustness is due to the fact that the spore

[a]Corresponding author: meike.mueller@dlr.de

DNA is protected by several dense coat layers and small acid soluble proteins.[10,11] For this reason, spores are used as model organisms to test the effectivity of different inactivation methods.[10]

In order to decontaminate spacecraft equipment, validated inactivation methods are needed. Today, dry-heat microbial reduction (DHMR) and vapour phase bioburden reduction using hydrogen peroxide (VHP) are evaluated sterilization methods for planetary protection missions by the European Cooperation for Space Standardization (ECSS).[12,13] Nevertheless, these technologies have a severe disadvantage: The sensitivity of modern instruments prohibits a complete sterilization of the spacecraft equipment.[3] In detail, ECSS reported in their standard,[14] that high temperatures could negatively affect heat sensitive materials and high concentrations of H_2O_2 could alter different materials (epoxy, silver, cellulose etc.).[14] In addition, copper, silver and manganese can lead to a catalytic decomposition of H_2O_2. Hence, new low-temperature sterilization technologies in addition to VHP and DHMR are required to treat various spacecraft components without damaging the surface. Furthermore the low-temperature sterilization technology should be compatible with materials used in space industry, and should provide an adequate microbial reduction.[2]

Sterilization using plasma comprises a plurality of benefits such as low cost, simple design and comfortable usage without organic residues after the treatment.[15] Cold atmospheric plasma (CAP) is one of the most promising low-temperature sterilization technologies.[16,17] Cold plasma at atmospheric pressure is a partially ionized gas which is not in thermal equilibrium as the temperature of its electrons is much higher than the temperature of its ions and neutrals.[18] It is often generated with helium and argon combined with a molecular gas like oxygen, but also ambient air can be used.[19,20] In principle the plasma technology allows direct and indirect ways of treatment. For the direct treatment, the visible plasma region is in contact with the target which is treated. As a result, short lifetime species with a high chemical activity, such as electrons and ions, reach the target. Additionally, the emitted UV light could inactivate microorganisms. For the indirect plasma treatment, only stable species with a long lifetime, e.g. O_3, H_2O_2, and NO_2, are able to reach the target. This cocktail of long-lifetime plasma species is called "plasma afterglow" and is predominant for the treatment of targets located at a certain distance from the plasma source.[21,22] Plasma technologies are already applied in various fields, for example for treatment of medical equipment, implants, and in the food industry.[23]

Various plasma sources have already been used for plasma decontamination:[24] Shimizu *et al.*,[10] Stapelmann *et al.*[25] and Cooper *et al.*[21] demonstrated that low pressure plasma, as well as atmospheric pressure plasma are both able to inactivate bacterial endospores. Each plasma technology has its own advantages and disadvantages. The plasma technologies, which are working with a direct treatment and UV-light, have difficulties to access narrow cavities or complex geometries. The afterglow plasma operates like a reactive gas and could penetrate in these areas per diffusion and convection. In general, low pressure plasmas are always bound to vacuum chambers. Thus, a scaling up of the device would lead to high costs. For CAPs, atmospheric pressure plasma jets (APPJs) and dielectric barrier discharge (DBD) plasmas are often used. In plasma jets, the plasma discharge is ignited inside a nozzle and transported outside using a gas flow.[26] APPJs are useful in decontamination of sensitive materials,[26] but the use of plasma jets requires a scanning process for the complete area as well as cavities because the plasma radiation area is often limited to only a few millimeters.[23] Furthermore, rare gas is often required for plasma production. In DBD plasma sources, the plasma is ignited between two electrodes, while one or both are covered with a dielectric layer.[27] In medical applications, in many cases the skin is one of the electrodes. DBDs could treat large surfaces, but the surface has to be flat to avoid inhomogeneous plasma discharges.[23]

In this study we continue the former work by Shimizu *et al.*[10] regarding the use of CAP for the decontamination of spacecraft components. Shimizu *et al.*[10] used an open system where the bacterial samples were treated with CAP afterglow transported by convection and diffusion. This setup has the drawback that it is an open system without plasma boosting.

We would like to overcome these drawbacks by using an indirect plasma treatment with a closed CAP afterglow circulation apparatus. The use of long-lifetime plasma species allows a homogeneous and gentle way of bacterial inactivation. The technology can be utilized under atmospheric conditions and has no requirement of expensive vacuum chambers.[28] Because the operation is below 40°C and at atmospheric pressure, it is possible to treat heat-sensitive materials, even living tissue.[28,29] In our closed CAP apparatus the afterglow is transported by an applied circulating flow – called "plasma

boosting." For the plasma production, a surface micro-discharge (SMD) electrode is used at ambient air.[20]

In this study, we introduce our designed, built and tested CAP circulation setup with variable treatment chamber volumes. Here, we use bacterial endospores of *Bacillus atrophaeus* as a biological indicator to test the sterilization efficacy depending on volume and treatment time. Three different sizes of treatment volumes were examined to demonstrate the scalability of the setup. We additionally analysed the afterglow components with UV absorption and a Fourier Transform Infrared spectrometer (FTIR) to identify the long-living reactive species which are responsible for the afterglow efficacy.

II. EXPERIMENTAL SETUP AND METHODS

A. Setup

The designed and tested decontamination apparatus consists of 1) a plasma source of two cylindrical electrodes to generate the CAP, 2) a treatment chamber, 3) an FTIR to investigate the composition of the afterglow species, 4) a humidifier for the circulating ambient air and 5) a membrane pump to create a circulating gas flow as shown in Fig. 1a). These components are connected by 6.35 mm (0.25″) tube fittings (Swagelok, Germany) and corresponding Perfluoroalkoxy alkanes (PFA) tubes (Swagelok, Germany) of 6.35 mm outer diameter and ~ 4 mm inner diameter. In addition, the connection to the gas washing bottle was achieved by silicone tubes of 6.3 mm inner diameter (VWR International GmbH, Germany). Previous studies showed that the inactivation efficacy of microorganisms increases with air humidity.[30] Based on this finding, the apparatus is operated under a relative humidity of approximately 90 % in ambient air at room temperature and under ambient pressure. The humidification is achieved by a 500 ml gas washing bottle (Carl Roth GmbH, Germany), filled with 400 ml distilled water. As demonstrated in Fig. 1a), the air passes through the water (bubbling) and becomes humid. The humidified air is transported to the electrode system by a membrane pump (KNF N86KT.18, Carl Roth GmbH, Germany) with a velocity of 3.5 l/min.

When the circulating air passes the electrode tubes (terraplasma GmbH, Germany), reactive oxygen and nitrogen species (RONS) are produced by micro-discharges of the plasma. The plasma afterglow is transported to the treatment chamber and through a heating pipe to the FTIR spectrometer (CX 4000, Gasmet Ansyco, Germany) to analyse the afterglow composition. The heating pipe of 1 m length and 60 °C is crucial to avoid condensation on the spectrometer mirrors. This leads to a temperature increase less than 2 °C in the treatment chamber over the maximum treatment time of 30 min. Therefore we assume that the afterglow composition is not affected. Finally, the afterglow gas returns into the humidifier and runs through the closed circuit again. Using a closed apparatus causes "plasma boosting" with high concentrations of reactive species. In this study, three different volumes (0.54 l, 1.80 l and 2.6 l) of air-tight aluminium boxes were used as treatment chambers.

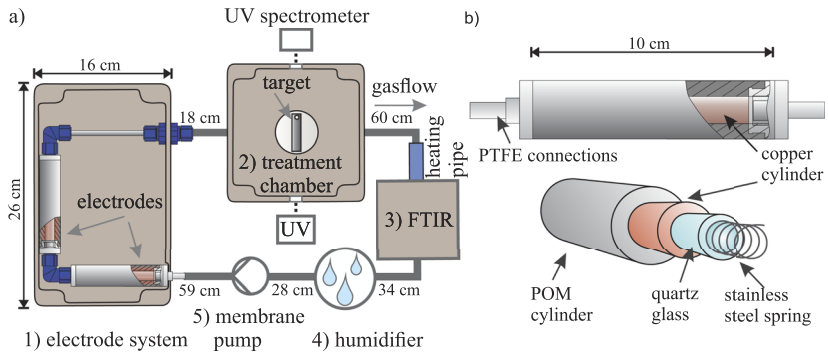

FIG. 1. a) Plasma afterglow circulation apparatus consisting of an electrode box with two SMD electrodes, treatment chamber, FTIR, humidifier and membrane pump. The stainless steel target is placed in the middle of the treatment chamber at the bottom. The in- and outflow of the afterglow is achieved via openings with 4 mm diameter in the middle of the side walls. b) Structure of the SMD electrodes with cylindrical shape.

The samples are placed at the bottom of the treatment chamber, so that they are not in the direct line of the afterglow flow. The reactive gas enters the treatment chamber in the middle of the sidewall (in a height of 36 mm/41 mm/46 mm for the treatment volumes 0.54 l/1.8 l/2.6 l) through a round opening with 4 mm diameter and fills up the volume of the treatment chamber. The maximal residual system volume was estimated with 250 ml without FTIR and 700 ml with FTIR, respectively. For the use of the FTIR, there is no need to remove gas from the system, but the spectrometer increases the total volume of the apparatus about 450 ml, because the gas has to fill up the measuring cell.

Fig. 1b) shows a sketch of the electrodes for plasma production based on the surface micro-discharge (SMD) plasma technology.[15,20]

In our setup, the surface micro-discharge (SMD) plasma electrode has a coaxial structure. One SMD electrode consists of a grounded stainless steel electrode with spring shape, which is separated by a quartz glass tube covered by a driven copper electrode as shown in Fig. 1b). The electrode tube has an inner diameter of 12 mm and a length of 100 mm. The SMD electrodes are enclosed in a sealed Polyoxymethylene (POM) cylinder with PTFE connections to the plasma region. For the plasma generation, a high voltage amplifier (Trek, 10/10B HS, Acal BFi Germany GmbH, Germany) and a function generator (Hameg, HM8150, Hameg Industries, Germany) are used to apply a high sinusoidal voltage (10 kHz, 6.4 kV_{pp}) to the electrode. The applied high voltage generates numerous micro-discharges on the side of the stainless-steel spring which partly ionize the circulating gas. The activated gas molecules react and form the long-living reactive species of the plasma afterglow which is used for the sporicidal inactivation.

To gain perception of the reaction mechanisms of the SMD afterglow plasma, the reactive gas was characterized, using a FTIR and UV absorption spectroscopy. In addition to the spectroscopic analysis of the afterglow using FTIR, the O_3 concentration is monitored by UV absorption at 254 nm wavelength using a spectrometer and a UV lamp (STS-UV, Ocean Optics, Germany). For this purpose, the spectrometer is positioned at the treatment chamber to measure the O_3 concentration directly inside the chamber. For the estimation of the ozone concentration, we used the absorption cross section[31] of 1.147 x 10^{-17} cm^2 at 254 nm wavelength. For the investigation of the dissolved molecules in the water of the wash bottle a UV/VIS spectrometer (Lambda 35, PerkinElmer, Germany) was used. To control the reproducibility of the afterglow generation, the dissipated plasma power is monitored. The plasma power consumption is determined by using voltage-charge-cyclograms (Lissajous figures).

B. Measurement of sporicidal effect

In the first investigations with the newly developed CAP circulation setup we analysed the efficacy of the sporicidal inactivation. Here, *Bacillus atrophaeus* spores ATCC 9372 dried on stainless steel plates (V4A) of 30 × 5 mm^2 were used as biological indicators with an initial number of spores $N_0 \sim 10^6$ cfu/target (cfu: colony forming units). The biological indicators were produced and packed in Tyvek for storage by SIMICON GmbH (Munich, Germany). For the discussion of the results we calculated the log reduction log (N_0/N), which referred to the inactivation of *Bacillus* in orders of magnitude. A reduction of ~ 6 log corresponds to the complete inactivation of all bacteria within the available measurement range with these spore samples. The treatment time for a 6 log reduction can be used to calculate the treatment time for a 12 log reduction (overkill procedure).[32] The bioburden on the target is considered zero after applying the overkill procedure.[12] The plasma treatment and the microbiological evaluation protocol are presented as follows:

1. The apparatus was activated for 20 min before the CAP treatment to stabilize the temperature, the concentration of reactive species and humidity in the system. The gas flow rate was 3.5 l/min and the relative humidity in the system about 90 %. Note that the CAP was already produced in this heat-up preparation of the electrodes.
2. After the heating phase of 20 min, the pump was switched-off and the treatment chamber was opened, so that the reactive gas of the treatment chamber exchanged with the environmental air. The residue reactive species remained in the tubes of the apparatus. Afterwards, the biological samples were placed on the bottom in the middle of the treatment chamber before the treatment chamber was closed.

3. The samples were treated by the SMD plasma gas (f = 10 kHz, U = 6.4 kV_{pp}) for the chosen treatment time without Tyvek. The treatment times for the 0.54 l treatment chamber were 2.5, 5.0, 7.5 and 10 minutes, for the 1.8 l chamber 2.5, 5.0, 7.5, 15 and 20 minutes and for the 2.6 l chamber 2.5, 5.0, 10, 15, 20 and 30 minutes. When the plasma treatment was started, the pump was switched-on again.
4. After the plasma treatment, plasma and gas flow were switched-off and the samples were transferred into 15 ml centrifuge tubes filled with 5 ml highly purified water (Ampuwa, Fresenius Kabi AG, Germany).
5. The samples were washed out using a vortex mixer for 1 min, an ultra-sonic bath for 30 min, a vortex mixer for 1 min, a ultra-sonic bath for 15 min and again a vortex mixer for 1 min.
6. Another 5 ml of highly purified water was added to the tubes and a dilution series up to $1{:}10^4$ was prepared. 100 µl of each suspension was plated on Müller-Hinton (OXOID, Germany) agar plates and incubated overnight at 37 °C.
7. In parallel to 6., the rest of the suspension was filtered using a membrane filter (0,47µm, Merck KGaA, Germany). The filter was incubated on Müller-Hinton agar plates overnight at 37 °C. By this procedure, the inactivation of spores up to 6 log could be proved.
8. At least nine spore samples were treated to obtain one data point. The measurements for one data point were performed at least on three different days. For each data point, three control samples without any treatment were used to determine the initial number of spores N_0 which were deposited on the stainless steel surface. To determine the number N_0 of cfu of the control samples, three untreated samples were transferred into separate centrifuge tubes and the microbiological protocol was executed (4.-7.).
9. By counting cfu on each plate, the number of survived spores by the plasma treatment N and untreated controls N_0 were estimated.

The error bars for the investigation of the inactivation were calculated using error propagation with standard deviations of the measurement series. They are presented only upwards to improve the readability of the semi logarithmic view. For the inactivation measurements, the FTIR was not included in the circulation system.

III. RESULTS AND DISCUSSION

A. Plasma characteristics

Fig. 2 shows the electrodes' power consumption and the H_2O gas - concentration measured for the 1.8 l treatment chamber as a function of time. The black line shows the heat-up phase, where the plasma ignition removes remaining precipitates and water on the surface of the electrodes. This removal of precipitates leads to a rapid increase of the power consumption in the first minute. The rise of the electrode temperature induces the subsequent decrease of the power consumption after

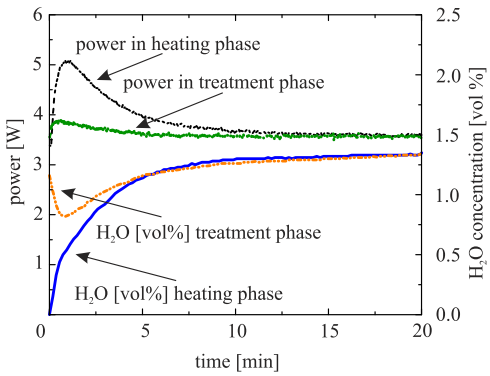

FIG. 2. Dissipated plasma power in the heating phase (black line). Dissipated plasma power in the treatment phase (green line). Development of H_2O concentration in the heating phase (blue line). Development of H_2O concentration in the treatment phase (orange line).

1 min. Furthermore, Fig. 2 shows the power consumption of a treatment phase, when the electrode is already heated up. The plasma is switched of for ~ 5 min between the different phases to put in the spore samples. The first increase of the power consumption is lower in the treatment phase than in the heating phase. In both cases, the power consumption reaches the threshold value 3.6 W after 20 min. The solid line shows the H_2O concentration, measured with the FTIR, during the heating phase. We observe that the apparatus needs up to 10 min to operate in a stable moisture condition. The H_2O concentration decreases in the beginning of the treatment phase, because the treatment chamber was opened to put in the spore samples. The open treatment chamber causes an exchange of humid and dry air. To minimize the loss of humid air, the gas flow is interrupted for the opening.

As already mentioned, previous studies show that the inactivation efficacy for microorganisms using cold plasma increases with increasing air humidity.[30] It is assumed that the production of hydroxyl radicals leads to this observation.[30] Our results illustrate that it is important to include a 20 min heating phase to achieve reproducible results.

As ozone is one of the dominant species produced by SMD plasmas using ambient air, and as it is known as an oxidizing and bactericidal agent.[33,34] The ozone concentrations were measured in the middle of the treatment chambers with three different volume sizes (0.54 l, 1.80 l, 2.60 l) by using UV absorption. Fig. 3 shows the O_3 concentration in the treatment phase as a function of time. The data points represent the average of six measurements which were recorded on three different days to consider possible variations. The error bar in Fig. 3 shows the maximum standard deviation of the measurements (approx. 50 ppm). The standard deviation is varying with the treatment time. To obtain clearance of the diagram, only the maximum standard deviation error bar is shown. The data show that the O_3 concentration increases in the three chambers with different rates in the first five minutes. Afterwards, the O_3 concentration saturates in each treatment chamber at values of about 600 ppm. The O_3 filling rate in the 0.54 l chamber is higher than for the larger treatment chambers because the ozone production rate by the SMD electrodes is constant. For $t > 10$ min, the production of ozone is balanced with the recombination in the setup, so that the concentration reaches a plateau. The filling rates of the apparatus were calculated with linear fits in Fig. 3 (R^2 values of the linear fits: 0.54l: 0.9987, 1.8 l: 0.9998, 2.6 l: 0.9985). The O_3 concentration increases with the filling rate of 360 ppm/min in the 0.54 l volume, with 203 ppm/min in the 1.8l volume and with 161 ppm/min in the 2.60 l volume. The filling rates were calculated with the data of the first 30 s, because the recombination rates increase with the concentration of the reactive species which lead to a non-linear development.

B. Sporicidal effect

The spore samples were placed at the bottom in the middle of the treatment chamber and were exposed to the afterglow for various treatment times. At least nine spore samples were treated to

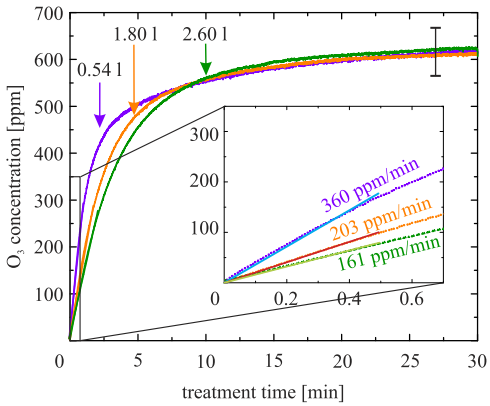

FIG. 3. Ozone concentrations in three different treatment volumes of 0.54 l, 1.80 l and 2.60 l during the treatment phase (after the heating phase). The error bar represents the maximum standard deviation of the measurements.

obtain one data point. For each data point, three control samples without any treatment were used to determine the initial number of spores N_0 which were deposited on the stainless steel surface, as described in Sec. II B. Afterwards, the survival rates N/N_0 were calculated for each experiment. Fig. 4 represents the mean value of the survival rates over the experiments for all treatment days for different treatment times using three treatment chambers. We find an increase of the inactivation rate of the spores with the increase of exposure time to the CAP afterglow. The investigations illustrate that the inactivation is faster in the smaller volume. A 4.6 log reduction was reached after 10 min treatment in 0.54 l and a 4.4 log reduction was realized after 20 min in 1.8 l treatment volume. In the largest volume of 2.6 l, 30 min were required to observe a log reduction of 4.6. The exponential fits (0.54 l: 0 – 10 min; 1.8 l: 0-15 min; 2.6 l: 0-20 min) in Fig. 4 emphasise the different inactivation efficacies of the used treatment chambers in the first minutes. Here, we calculated the D-values for different treatment volumes using the functions of the exponential fits in Fig. 4 D value = 2.0 min for 0.54 l, D value = 3.7 min for 1.8 l and D value = 4.8 min for 2.6 l (R^2 values of the exponential fits: 0.54 l: 0.984, 1.8 l: 0.995, 2.6 l: 0.965). The survival rate N/N_0 in Fig. 4 demonstrates a fast sporicidal inactivation at the beginning which turns into a slower inactivation after a survival rate of $\sim 10^{-4}$ (4 log).

A plausible explanation for the slower decrease of the survival rate $< 10^{-4}$ in Fig. 4 is the formation of spore multi-layers on the target.[35] By the plasma treatment, the top layer of spores is inactivated first, while the inactivation of the layers below is limited because they are at least partly covered by other spores.[35] This multi-layer formation leads to a wide variation of inactivation efficacy among different target samples. This idea is supported by an SEM image of the (untreated) spore samples shown in Fig. 5. The spores are inhomogenously distributed over the stainless steel plate, so that areas with spore multilayers and empty areas are observed in the SEM image. This confirms the theory that the spores are not homogeneously spread over the surface but form spore-clusters which could lead to a multilayer formation (Fig. 5a)). Fig. 5b) presents the multilayers with increased magnification. Table I summarizes the comparison of the treatment methods of ECSS standard, Shimizu *et al.*[10] and the present study.

ECSS propose for > 4 log bioburden reduction a minimum temperature of 125 °C. The VHP treatment time for bioburden reduction depends on the H_2O_2 concentration. For example, with an H_2O_2 concentration of 1 mg/L, the D-value is 3.3 min. The data presented here demonstrate that the new designed apparatus needs less than a 30 min treatment time to achieve a 4.4 log reduction for endospores. Additional to the previous mentioned studies in the introduction, CAP already showed its inactivation effect on microorganisms. Mandler *et al.*[36] already used a similar apparatus to demonstrate the inactivation of *E. mundtii* on stainless steel and dental equipment. In contrast to the work presented here, a small treatment volume was sufficient, and the composition of the reactive species were not analysed in detail.

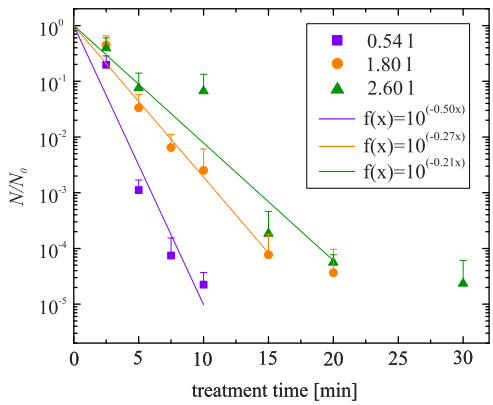

FIG. 4. Survival rates of *Bacillus atrophaeus* spores treated in different treatment volumes as a function of treatment time. The error bars were calculated using error propagation with standard deviations of the measurement series. They are presented only upwards to improve the readability of the semi logarithmic view.

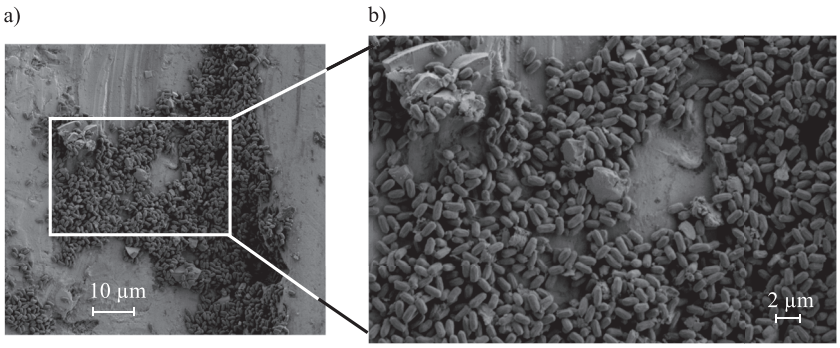

FIG. 5. SEM image of the spore sample of SIMICON GmbH. a) The SEM image of a spore sample demonstrates the multilayer formation or clumping of *B. atrophaeus* in some parts of the samples, while other sample areas are not covered. b) SEM image with increased magnification shows the accumulation of the spores.

Recent studies also investigated the effect of cold atmospheric air plasma on *Bacillus* spores for different plasma devices. Kuzminova *et al.*[37] reported in their study that *B. subtilis* spores could almost completely be etched by DBD plasma within a few minutes. But they also observed an etching effect of polymers by the DBD plasma. Reineke *et al.*[38] and van Brokhorst-van de Veed *et al.*[39] demonstrated an inactivation of bacterial endospores using an atmospheric pressure plasma jet. In principal, plasma jets are effective devices to inactivate various microorganisms. But the application is limited so a small treatment area which impedes the treatment of large objects. Klämpfl *et al.*[28] used the SMD technology to rapidly inactivate different *Bacillus* species. The SMD electrode was positioned close to the samples and operated in a smaller volume than the presented apparatus. Beside the reactive ROS and RNS, electrical forces could have affected the inactivation process.

Since the plasma afterglow could provide a more sensitive surface application, longer treatment times are necessary, but the material compatibility is supposed to be higher. The big advantage is that the reactive afterglow can be used in a defined treatment volume and the afterglow can diffuse into narrow cavities. Further investigations have to be executed to analyse the efficiency of the inactivation of 3D objects. It is supposable, that the treatment volume could exceed the largest tested treatment chamber of 2.6 l by extending the treatment time or using multiple SMD electrodes to fill up the treatment chamber.

Fig. 6 shows the survival rate of *Bacillus atrophaeus* as a function of the applied ozone dose (integrated O_3 concentration in Fig. 3). The spore survival rates decrease with increasing ozone dose in all treatment volumes. This supports the hypothesis that the inactivation depends on the present ozone concentration and that ozone is an important inactivation agent in our experiment.[33,40]

Previous studies already reported about the sporicidal effect of gaseous ozone.[41,42] Aydogan *et al.*[41] reported a 3 log reduction of *B. subtilis* spores for a O_3 concentration of 3 mg/l (~1500 ppm) after 4 hours exposure time with 90 % relative humidity and an associated D value of 43 min. Ishizaki *et al.*[42] received a maximum D value of 20 min for 3 mg/l (~1500 ppm) and 90 % relative humidity.

TABLE I. Comparison of the treatment methods of ECSS standard, Shimizu *et al.* and this study.

Method	Temperature [°C]	Treatment time [h]	Log Reduction	Target
DHMR ECSS[13]	125	35.4	4	Bioburden reduction
	170	0.42	4	Bioburden reduction
SMD Shimizu *et al.*[10]	25	1.5	3 - 4	*B. atrophaeus*
SMD present study	22	< 0.5	> 4.4	*B. atrophaeus*
VHP (controlled ambient environment)[12] H_2O_2 concentration > 1.1 mg/L	25- 45	200 (mg/L)sec	1	Bioburden reduction
VHP (controlled vacuum conditions)[12] H_2O_2 concentration > 0.5 mg/L and < 1.1 mg/L	25- 45	200 (mg/L)sec	1	Bioburden reduction

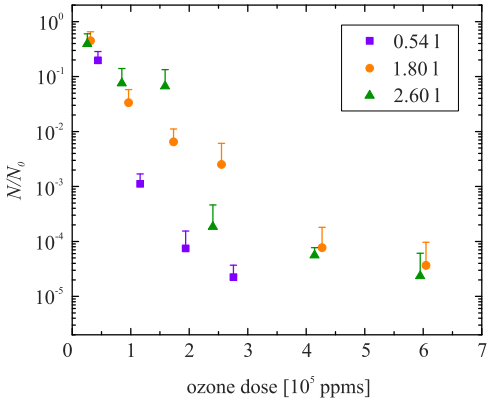

FIG. 6. Survival rate of *B. atrophaeus* spores as a function of O_3 dose for different treatment volumes. The error bars were calculated using error propagation with standard deviations of the measurement series. They are presented only upwards to improve the readability of the semi logarithmic view.

Compared to the present study, the research of Aydogan *et al.* and Ishizaki *et al.* indicate that ozone is not the only inactivating agent in the developed apparatus, because the measured D values are 2.0 - 4.8 min.

In addition, Shimizu *et al.*[10] investigated the inactivation rate of *B. atrophaeus* by the plasma afterglow using SMD technology, for different plasma powers. They observed that the inactivation couldn't be explained only by the ozone concentration, because the inactivation rate was higher for lower ozone concentrations, than for higher ones. These studies indicate that ozone is not the only responsible component for the inactivation of microorganisms using the plasma afterglow.

Next, we shall analyse the plasma chemistry in more detail.

C. Plasma chemistry analysis

Numerical simulations predict that O_3, NO_2, N_2O, N_2O_5, HNO_2, HNO_3 and H_2O_2 are long-living reactive species produced by SMD.[33,34] The detailed mechanisms of the coupled, dynamic processes in the SMD plasma are poorly understood.[34] Pavlovich *el al.*[43] identified ozone O_3, nitrous oxide N_2O, nitric oxide NO and nitrogen dioxide NO_2 as prominent components in SMD air plasma chemistry. Furthermore, they observed that the concentration of nitric acid HNO_3 fluctuated with time and power density. Their explanation for this observation is that HNO_3 is sensitive to ambient water vapour concentrations.

Since our apparatus was operated under high humidity conditions of ~ 90 % relative humidity (RH) and with a circulating gas flow, the composition of the afterglow was analysed with an FTIR to gain insights into the inactivation process. Fig. 7 shows the analysed absorption spectra of the

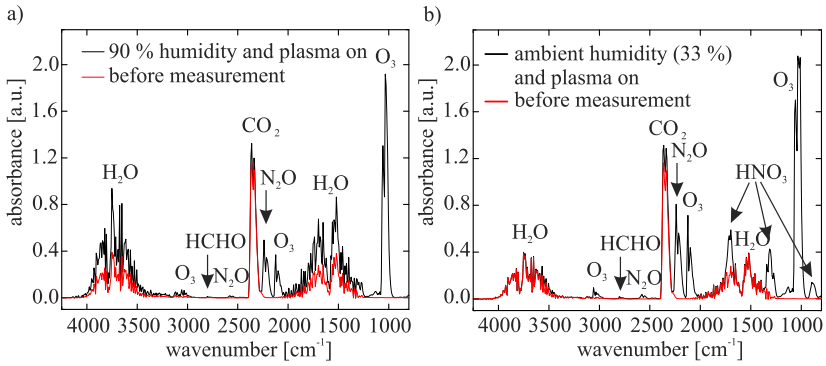

FIG. 7. FTIR absorption spectra: a) Absorption spectra before plasma ignition (red line) and during plasma ignition with high humidity conditions ~ 90 % RH (black line). b) Absorption spectra before plasma ignition (red line) and during plasma ignition with ambient humidity condition ~ 33 % RH (black line).

afterglow plasma as a function of the wavenumber in a range of 850 cm^{-1} - 4200 cm^{-1}. To minimize the loss of reactive species the plasma source was connected to the FTIR without the treatment chamber in the cycle. The afterglow gas has to pass the distance of 1 m heating pipe before it is analysed by the FTIR. The reduction of the reactive species with this distance is supposed to be low, because the gas is transported with 3.5 l/min to the analyser and the circulation of the afterglow leads to a homogeneous distribution of the reactive species in the circulation system. This data was recorded for ambient humidity conditions of ~ 33 % RH and for high humidity conditions of ~ 90% RH. Fig. 7a) presents the IR absorption spectrum before plasma ignition with ambient humidity conditions and during plasma ignition with high humidity after 9.5 min treatment time. The time point 9.5 min was chosen as an exemplary treatment time point using the FTIR. The spectra indicate that CO_2, H_2O and N_2O are present in the treatment setup together with O_3. CO_2 and H_2O are components of the ambient air and not generated by the plasma. The absorbance by H_2O is increased under high humidity conditions. N_2O is produced by SMD plasma in a concentration of ~100 ppm. The concentrations of NO and NO_2 were below 1.3 ppm and not visible in Fig. 7a). Fig. 7b) shows the spectrum before plasma ignition as demonstrated in a) and the absorption spectrum during the plasma is on at ambient humidity conditions after 9.5 min. Similar to a), N_2O and O_3 are visible in the spectrum but in addition HNO_3 is detectable with the FTIR (75 ppm). Furthermore, the concentrations of the species are slightly higher than during high humidity conditions (N_2O: 200ppm). The reduction of the species concentration with moisture could be due to the use of the wash bottle as a humidifier, which could cause dissolving of molecules in water. The study of Oehmigen *et al.*[44] reported that no sporicidal effect of HNO_3 could be detected for *B. atrophaeus* after 2h incubation.

Fig. 8a) shows the concentration of ozone O_3 and nitrate NO_3 for different treatment times and Fig. 8b) the measured UV absorption spectrum of the water. We analysed the absorbance for nitrate at 205 nm with molecular absorption coefficient[45] of 38750 $M^{-1}cm^{-1}$ and for O_3 at 260 nm with molecular absorption coefficient[46] 3300 $M^{-1}cm^{-1}$ with Lambert-Beer. The molecular absorption coefficient of nitrate was calculated with the data of Edwards *et al.*[45] For the detection of the UV spectrum the water was treated with plasma for duration of 65 min. The plasma-treatment was interrupted for ~5 min at the time points 20 min, 35 min and 50 min to detect the absorption spectrum. The measurements of the UV spectrum were repeated after 1 min for each time point. The analysis indicates that ozone and nitrate were dissolved in the water of the wash bottle. The ozone concentration doesn't increase over time due to its high activity. The repeated measurements ~ 1 min after the first measurement indicate that the ozone concentration decrease fast after the plasma treatment. NO_3 is more stable in water and increases over time. The detection of nitrate agrees with the assumption that HNO_3 is dissolved in water under high humidity conditions.

It is crucial to measure the reactive species in the CAP to optimize the microbial inactivation in this newly designed and tested apparatus. We do not come to a conclusion what reactive species are responsible for the inactivation of microorganisms but O_3 and N_2O seem to be major measurable

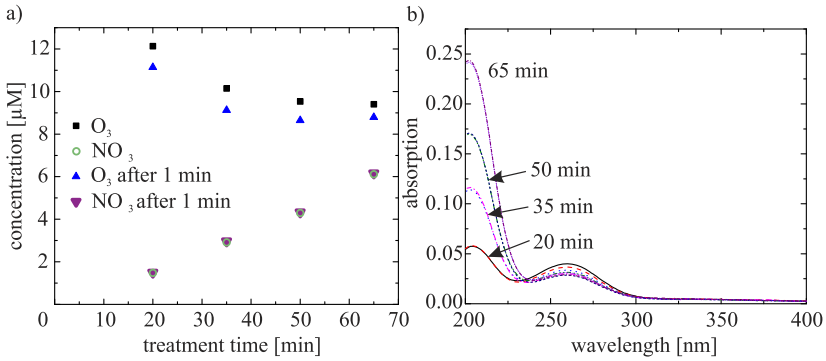

FIG. 8. a) Concentrations of O_3 and NO_3 which are solved in water in the gas washing bottle for different treatment times. The repetition of the measurements after 1 min demonstrates the fast decay of O_3 in water. b) UV/Vis absorption spectrum of the water in the gas washing bottle after different treatment times.

TABLE II. Log reduction for different treatment times in different treatment volumes.

Treatment volume [l]	Treatment time [min]	Log reduction
0.54	10	4.6
1.8	20	4.4
2.6	30	4.6

components of the reactive gas mixture under high humidity conditions. Further investigations are needed to study the relation between the distribution of reactive species and the inactivation of bacterial endospores.

IV. CONCLUSION AND OUTLOOK

The presented plasma afterglow circulation apparatus was designed, built and investigated for the decontamination of spacecraft equipment. With the presented setup, 4.4 - 4.6 log reductions of *B. atrophaeus* spores were achieved for different treatment volumes of 0.54 l, 1.8 l and 2.6 l (presented in Table II).

The results in Table II show that the newly developed CAP apparatus very efficiently inactivated bacterial endospores inoculated on stainless steel. The measurements of the O_3 concentration support the hypothesis that ozone itself plays an important role in the inactivation process of *B. atrophaeus* but previous studies of Ishizaki *et al.* and Aydogan *et al.* emphasize that the effect of ozone alone could not explain the measured D values in the present study. The first FTIR and UV absorption measurements identified nitrogen oxides as possible important components for inactivation - in addition to O_3.

The newly developed circulation setup offers a useful inactivation method in an easily scalable system for targets with flat surfaces without causing high costs. Vacuum systems and the use of rare gases are not necessary. One of the next steps will be the testing of the inactivation efficacy of the apparatus for 3D objects and packed treatment targets. The apparatus works at ambient pressure and room temperature, with reactive species transported via gas flow to the sample area. The results furthermore show that the mechanism of inactivation of bacterial endospores is still not fully understood. Further FTIR investigations are required to examine the responsible plasma species in the presented setup in relation to humidity for inactivation of endospores.

In addition, material compatibility analysis for aerospace relevant materials will be executed to examine the applicability of the new CAP apparatus for planetary protection. However, one can clearly conclude, the CAP based on the SMD technology is a promising alternative method for inactivation of microorganisms for spacecraft equipment without the need for destructively high temperatures. Since CAP is already used in the medical field for sensitive surfaces like skin[29] and for decontamination of food,[47] we assume, that the technology could also be applied for sensitive materials which are not compatible with H_2O_2. Detail material compatibility tests will be executed in a follow-up study.

ACKNOWLEDGMENTS

We would like to acknowledge the financial support of Bayrisches Wirtschaftsministerium. The authors also would like to acknowledge Matthias Kolbe of Deutsches Zentrum für Luft-und Raumfahrt, Institut für Materialphysik im Weltraum for the SEM measurement.

[1] "COSPAR's planetary protection policy," Space Research Today **200**, 12–25 (2017).
[2] T. Pottage, S. Macken, K. Giri, J. T. Walker, and A. M. Bennett, "Low-temperature decontamination with hydrogen peroxide or chlorine dioxide for space applications," Applied and Environmental Microbiology **78**(12), 4169–4174 (2012).
[3] C. Moissl-Eichinger, P. Rettberg, and R. Pukall, "The first collection of spacecraft-associated microorganisms. A public source for extremotolerant microorganisms from spacecraft assembly clean rooms," Astrobiology **12**(11), 1024–1034 (2012).
[4] C. Moissl-Eichinger, A. K. Auerbach, A. J. Probst, A. Mahnert, L. Tom, Y. Piceno, G. L. Andersen, K. Venkateswaran, P. Rettberg, S. Barczyk, R. Pukall, and G. Berg, "Quo vadis? Microbial profiling revealed strong effects of cleanroom maintenance and routes of contamination in indoor environments," Scientific Reports **5**, 9156 (2015).
[5] M. Stieglmeier, P. Rettberg, S. Barczyk, M. Bohmeier, R. Pukall, R. Wirth, and C. Moissl-Eichinger, "Abundance and diversity of microbial inhabitants in European spacecraft-associated clean rooms," Astrobiology **12**(6), 572–585 (2012).

[6] C. Moissl-Eichinger, R. Pukall, A. J. Probst, M. Stieglmeier, P. Schwendner, M. Mora, S. Barczyk, M. Bohmeier, and P. Rettberg, "Lessons learned from the microbial analysis of the Herschel spacecraft during assembly, integration, and test operations," Astrobiology **13**(12), 1125–1139 (2013).
[7] K. Koskinen, P. Rettberg, R. Pukall, A. Auerbach, L. Wink, S. Barczyk, A. Perras, A. Mahnert, D. Margheritis, G. Kminek, and C. Moissl-Eichinger, "Microbial biodiversity assessment of the European Space Agency's ExoMars 2016 mission," Microbiome **5**(1), 143 (2017).
[8] P. Schwendner, C. Moissl-Eichinger, S. Barczyk, M. Bohmeier, R. Pukall, and P. Rettberg, "Insights into the microbial diversity and bioburden in a South American spacecraft assembly clean room," Astrobiology **13**(12), 1140–1154 (2013).
[9] D. L. Nuding, R. V. Gough, K. J. Venkateswaran, J. A. Spry, and M. A. Tolbert, "Laboratory investigations on the survival of Bacillus subtilis spores in deliquescent salt Mars analog environments," Astrobiology **17**(10), 997–1008 (2017).
[10] S. Shimizu, S. Barczyk, P. Rettberg, T. Shimizu, T. Klaempfl, J. L. Zimmermann, T. Hoeschen, C. Linsmeier, P. Weber, G. E. Morfill, and H. M. Thomas, "Cold atmospheric plasma—A new technology for spacecraft component decontamination," Planetary and Space Science **90**, 60–71 (2014).
[11] A. O. Henriques and C. P. Moran, "Structure, assembly, and function of the spore surface layers," Annual Review of Microbiology **61**, 555–588 (2007).
[12] European Cooperation for Space Standardization, "ECSS-Q-ST-70-56C vapour phase bioburden reduction for flight hardware," ECSS (2013).
[13] European Cooperation for Space Standardization, "ECSS-Q-ST-70-57C dry heat bioburden reduction for flight hardware" (2013).
[14] European Cooperation for Space Standardization, "ECSS-Q-ST-70-53C materials and hardware compatibility tests for sterilization processes" (2008).
[15] T. Shimizu, J. L. Zimmermann, and G. E. Morfill, "The bactericidal effect of surface micro-discharge plasma under different ambient conditions," New J. Phys. **13**(2), 023026 (2011).
[16] S. Lerouge, M. R. Wertheimer, and L. Yahia, "Plasma sterilization: A review of parameters, mechanisms, and limitations," Plasmas and Polymers **6**(3), 175–188 (2001).
[17] M. Laroussi, "Sterilization of contaminated matter with an atmospheric pressure plasma," IEEE Trans. Plasma Sci. **24**(3), 1188–1191 (1996).
[18] C. Hertwig, N. Meneses, and A. Mathys, "Cold atmospheric pressure plasma and low energy electron beam as alternative nonthermal decontamination technologies for dry food surfaces. A review," Trends in Food Science & Technology **77**, 131–142 (2018).
[19] G. Fridman, M. Peddinghaus, M. Balasubramanian, H. Ayan, A. Fridman, A. Gutsol, and A. Brooks, "Blood coagulation and living tissue sterilization by floating-electrode dielectric barrier discharge in air," Plasma Chem Plasma Process **26**(4), 425–442 (2006).
[20] G. E. Morfill, T. Shimizu, B. Steffes, and H.-U. Schmidt, "Nosocomial infections—A new approach towards preventive medicine using plasmas," New J. Phys. **11**(11), 115019 (2009).
[21] M. Cooper, G. Fridman, D. Staack, A. F. Gutsol, V. N. Vasilets, S. Anandan, Y. I. Cho, A. Fridman, and A. Tsapin, "Decontamination of surfaces from extremophile organisms using nonthermal atmospheric-pressure plasmas," IEEE Trans. Plasma Sci. **37**(6), 866–871 (2009).
[22] G. Fridman, A. D. Brooks, M. Balasubramanian, A. Fridman, A. Gutsol, V. N. Vasilets, H. Ayan, and G. Friedman, "Comparison of direct and indirect effects of non-thermal atmospheric-pressure plasma on bacteria," Plasma Process. Polym. **4**(4), 370–375 (2007).
[23] M. G. Kong, G. Kroesen, G. Morfill, T. Nosenko, T. Shimizu, J. van Dijk, and J. L. Zimmermann, "Plasma medicine. An introductory review," New J. Phys. **11**(11), 115012 (2009).
[24] P. Puligundla and C. Mok, "Inactivation of spores by nonthermal plasmas," World Journal of Microbiology & Biotechnology **34**(10), 143 (2018).
[25] K. Stapelmann, M. Fiebrandt, M. Raguse, P. Awakowicz, G. Reitz, and R. Moeller, "Utilization of low-pressure plasma to inactivate bacterial spores on stainless steel screws," Astrobiology **13**(7), 597–606 (2013).
[26] K.-D. Weltmann, R. Brandenburg, T. von Woedtke, J. Ehlbeck, R. Foest, M. Stieber, and E. Kindel, "Antimicrobial treatment of heat sensitive products by miniaturized atmospheric pressure plasma jets (APPJs)," J. Phys. D: Appl. Phys. **41**(19), 194008 (2008).
[27] S. U. Kalghatgi, G. Fridman, M. Cooper, G. Nagaraj, M. Peddinghaus, M. Balasubramanian, V. N. Vasilets, A. F. Gutsol, A. Fridman, and G. Friedman, "Mechanism of blood coagulation by nonthermal atmospheric pressure dielectric barrier discharge plasma," IEEE Trans. Plasma Sci. **35**(5), 1559–1566 (2007).
[28] T. G. Klämpfl, G. Isbary, T. Shimizu, Y.-F. Li, J. L. Zimmermann, W. Stolz, J. Schlegel, G. E. Morfill, and H.-U. Schmidt, "Cold atmospheric air plasma sterilization against spores and other microorganisms of clinical interest," Applied and Environmental Microbiology **78**(15), 5077–5082 (2012).
[29] G. E. Morfill, M. G. Kong, and J. L. Zimmermann, "Focus on plasma medicine," New J. Phys. **11**(11), 115011 (2009).
[30] M. Hähnel, T. von Woedtke, and K.-D. Weltmann, "Influence of the air humidity on the reduction of Bacillus spores in a defined environment at atmospheric pressure using a dielectric barrier surface discharge," Plasma Process. Polym. **7**(3-4), 244–249 (2010).
[31] J. Orphal and K. Chance, "Ultraviolet and visible absorption cross-sections for HITRAN," Journal of Quantitative Spectroscopy and Radiative Transfer **82**(1-4), 491–504 (2003).
[32] T. von Woedtke and A. Kramer, "The limits of sterility assurance," GMS Krankenhaushygiene Interdisziplinar (3), 3 (2008).
[33] T. Shimizu, Y. Sakiyama, D. B. Graves, J. L. Zimmermann, and G. E. Morfill, "The dynamics of ozone generation and mode transition in air surface micro-discharge plasma at atmospheric pressure," New J. Phys. **14**(10), 103028 (2012).
[34] Y. Sakiyama, D. B. Graves, H.-W. Chang, T. Shimizu, and G. E. Morfill, "Plasma chemistry model of surface microdischarge in humid air and dynamics of reactive neutral species," J. Phys. D: Appl. Phys. **45**(42), 425201 (2012).

[35] H. Shintani and A. Sakudo, eds., *Gas plasma sterilization in microbiology. Theory, applications, pitfalls and new perspectives* (Caister Academic Press, Norfolk, 2016).
[36] J. Mandler, S. Moritz, S. Binder, T. Shimizu, M. Müller, M. H. Thoma, and J. L. Zimmermann, "Disinfection of dental equipment—Inactivation of Enterococcus mundtii on stainless steel and dental handpieces using surface micro-discharge plasma," Plasma Med. **7**(4), 407–416 (2017).
[37] A. Kuzminova, T. Kretková, O. Kylián, J. Hanuš, I. Khalakhan, V. Prukner, E. Doležalová, M. Šimek, and H. Biederman, "Etching of polymers, proteins and bacterial spores by atmospheric pressure DBD plasma in air," J. Phys. D: Appl. Phys. **50**(13), 135201 (2017).
[38] K. Reineke, K. Langer, C. Hertwig, J. Ehlbeck, and O. Schlüter, "The impact of different process gas compositions on the inactivation effect of an atmospheric pressure plasma jet on Bacillus spores," Innovative Food Science & Emerging Technologies **30**, 112–118 (2015).
[39] H. van Bokhorst-van de Veen, H. Xie, E. Esveld, T. Abee, H. Mastwijk, and M. Nierop Groot, "Inactivation of chemical and heat-resistant spores of Bacillus and Geobacillus by nitrogen cold atmospheric plasma evokes distinct changes in morphology and integrity of spores," Food microbiology **45**(Pt A), 26–33 (2015).
[40] S. Pekárek, "Experimental study of surface dielectric barrier discharge in air and its ozone production," J. Phys. D: Appl. Phys. **45**(7), 075201 (2012).
[41] A. Aydogan and M. D. Gurol, "Application of gaseous ozone for inactivation of Bacillus subtilis spores," Journal of the Air & Waste Management Association **56**(2), 179–185 (2006).
[42] K. Ishizaki, N. Shinriki, and H. Matsuyama, "Inactivation of Bacillus spores by gaseous ozone," Journal of Applied Bacteriology **60**(1), 67–72 (1986).
[43] M. J. Pavlovich, D. S. Clark, and D. B. Graves, "Quantification of air plasma chemistry for surface disinfection," Plasma Sources Sci. Technol. **23**(6), 065036 (2014).
[44] K. Oehmigen, M. Hähnel, R. Brandenburg, C. Wilke, K.-D. Weltmann, and T. von Woedtke, "The role of acidification for antimicrobial activity of atmospheric pressure plasma in liquids," Plasma Process. Polym. **7**(3-4), 250–257 (2010).
[45] A. C. Edwards, P. S. Hooda, and Y. Cook, "Determination of nitrate in water containing dissolved organic carbon by ultraviolet spectroscopy," International Journal of Environmental Analytical Chemistry **80**(1), 49–59 (2001).
[46] E. J. Hart, K. Sehested, and J. Holoman, "Molar absorptivities of ultraviolet and visible bands of ozone in aqueous solutions," Anal. Chem. **55**(1), 46–49 (2002).
[47] N. N. Misra, X. Yepez, L. Xu, and K. Keener, "In-package cold plasma technologies," Journal of Food Engineering **244**, 21–31 (2019).